

# 1 Automated Pupillometry using a Prototype Binocular Optical 2 Coherence Tomography System

3  
4 Reena Chopra, BSc,<sup>1</sup> Pádraig J. Mulholland, PhD,<sup>1,2</sup> Axel Petzold, MD PhD,<sup>1,3</sup>, Lola  
5 Ogunbowale, FRCOphth FRCS FEBO,<sup>1</sup> Gus Gazzard, MD FRCOphth,<sup>1</sup> Fion  
6 Bremner, MBBS PhD FRCOphth,<sup>3</sup> Roger S. Anderson, PhD DSc,<sup>1,2</sup> Pearse A.  
7 Keane, MD FRCOphth<sup>1</sup>

8  
9 <sup>1</sup> NIHR Biomedical Research Centre for Ophthalmology, Moorfields Eye Hospital NHS Foundation  
10 Trust and UCL Institute of Ophthalmology, London, United Kingdom

11 <sup>2</sup> Centre for Optometry and Vision Science Research, School of Biomedical Sciences, Ulster  
12 University, Coleraine, United Kingdom

13 <sup>3</sup> Department of Neuro-Ophthalmology, National Hospital for Neurology and Neurosurgery, London,  
14 United Kingdom

## 15 16 Correspondence and reprint requests:

17 Pearse A. Keane, MD FRCOphth, NIHR Biomedical Research Centre at Moorfields Eye Hospital NHS  
18 Foundation Trust and UCL Institute of Ophthalmology, London, United Kingdom. Tel: +44 207 523  
19 3411 Fax: +44 207 566 2334 Email: [p.keane@ucl.ac.uk](mailto:p.keane@ucl.ac.uk)

## 20 Short title:

21 Automated, quantitative, pupillometry using Binocular OCT

## 22 23 Meeting Presentation:

24 This work has previously been presented at the ARVO Annual Meeting 2019 in Vancouver,  
25 Canada.

1  
2  
3  
4  
5  
6  
7  
8  
9  
10  
11  
12  
13  
14  
15  
16  
17  
18  
19  
20  
21  
22  
23  
24  
25  
26  
27  
28  
29  
30  
31  
32  
33  
34  
35  
36  
37  
38  
39  
40  
41  
42  
43  
44  
45  
46  
47  
48  
49  
50  
51  
52  
53  
54  
55  
56  
57  
58  
59  
60  
61  
62  
63  
64  
65

26 **Keywords:**

27 Binocular

28 Optical coherence tomography

29 Automated

30 Diagnostics

31 Pupils

32 Pupillometry

33 **Abbreviations:**

34 BA – Bland-Altman

35 CI – confidence interval

36 ICC – Intraclass correlation coefficient

37 MD – mean deviation

38 NTG – normal tension glaucoma

39 RANSAC – random sample consensus

40 OCT – optical coherence tomography

41 RAPD – relative afferent pupillary defect

42 SD – standard deviation

43 SFM – swinging flashlight method

44

45 **Words:**

46 3719

47

48 **Clips:**

49 This manuscript contains 1 video clip.

## Abstract

---

**Purpose:** To determine the test-retest reliability and diagnostic accuracy of a binocular optical coherence tomography (OCT) prototype (Envision Diagnostics, USA) for pupillometry.

**Design:** Assessment of diagnostic reliability and accuracy.

**Methods:** Fifty participants with RAPD confirmed using the swinging flashlight method (mean age 49.6 years) and 50 healthy controls (mean age 31.3 years) were examined. Participants twice underwent an automated pupillometry exam using a binocular OCT system that presents a stimulus and simultaneously captures OCT images of the iris-pupil plane of both eyes. Participants underwent a single exam on the RAPDx (Konan Inc, USA), an automated infrared pupillometer. Pupil parameters including maximum and minimum diameter, and anisocoria were measured. The magnitude of RAPD was calculated using the log of the ratio of the constriction amplitude between the eyes. A pathological RAPD was considered to be above  $\pm 0.5$  log units on both devices.

**Results:** Intraclass correlation coefficient was  $>0.90$  for OCT-derived maximum pupil diameter, minimum pupil diameter, anisocoria. The RAPDx had a sensitivity of 82% and a specificity of 94% for detection of RAPD whereas the binocular OCT had a sensitivity of 74% and specificity of 86%. The diagnostic accuracy of the RAPDx and binocular OCT was 88% (CI: 80-94%) and 80% (CI: 71-87%) respectively.

**Conclusions:** Binocular OCT-derived pupil parameters had excellent test-retest reliability. Diagnostic accuracy of RAPD was inferior to the RAPDx and is likely related to factors such as eye movement during OCT capture. As OCT becomes ubiquitous, OCT-derived measurements may provide an efficient method of objectively quantifying the pupil responses.

## 50 Introduction

51

---

52 Pupillometry is a valuable diagnostic tool to assess the integrity of the visual pathway and  
53 evaluate neurological function. The conventional method of assessing the pupil response is  
54 by shining a light into each eye while the responses are observed by the examiner's naked  
55 eye.

56 Relative afferent pupillary defects (RAPD) are often observed in asymmetric  
57 conditions affecting the retina, optic nerve or anterior aspects of the optic tract, where a  
58 lower magnitude of pupil constriction is observed when the light is swung from the affected  
59 eye to the unaffected eye. This method of clinical testing is known as the swinging flashlight  
60 method (SFM). The SFM requires a trained examiner and is known to be prone to error -  
61 subtle defects can be easily missed due to uneven illumination, or if the eye is stimulated off-  
62 axis<sup>1</sup>. Likewise, the interpretation of the SFM is difficult in the context of anisocoria, dark  
63 irides or poorly reacting pupils<sup>2</sup>. To address such issues, binocular pupillometers have been  
64 developed that can objectively quantify parameters of the pupil responses such as  
65 anisocoria, maximum and minimum pupil diameter, and dilation and constriction velocity<sup>3</sup>.  
66 These single-purpose instruments utilize infrared technology that can capture enface video  
67 images of the pupil without stimulating a response. In addition, the flash stimulus and testing  
68 environment is controlled, eliminating errors described above. Although these devices can  
69 provide objective data for the diagnosis and monitoring of neurological disease, SFM is still  
70 the method of choice in busy clinics due to its convenience and low-cost<sup>4</sup>.

71 Optical coherence tomography (OCT) devices are becoming ubiquitous in eye clinics  
72 to image ocular structures at micron-resolution. Anterior-segment OCT devices have  
73 previously been used to describe pupil parameters and iris dynamics for the study of  
74 accommodation<sup>5</sup> and anterior chamber dynamics for insight into primary angle closure<sup>6</sup>. In  
75 this report, we describe a new approach of measuring the pupil parameters and responses  
76 using an automated binocular optical coherence tomography (OCT) prototype device

1  
2  
3  
4  
5  
6  
7  
8  
9  
10  
11  
12  
13  
14  
15  
16  
17  
18  
19  
20  
21  
22  
23  
24  
25  
26  
27  
28  
29  
30  
31  
32  
33  
34  
35  
36  
37  
38  
39  
40  
41  
42  
43  
44  
45  
46  
47  
48  
49  
50  
51  
52  
53  
54  
55  
56  
57  
58  
59  
60  
61  
62  
63  
64  
65

77 (Envision Diagnostics, El Segundo, CA)<sup>7</sup>. This device acquires images of (in this case) the  
78 anterior segments, including the iris-pupil planes, of both eyes simultaneously while  
79 delivering a controlled light stimulus to either or both eyes on display screens within the  
80 device. The pupil parameters can thus be quantified to micrometer resolution precision using  
81 OCT technology that most eye care professionals are familiar with. In addition, the  
82 instrument's multi-purpose capabilities such as posterior segment imaging, visual acuity and  
83 visual field measurement, and ocular motility testing, could further increase the utility of the  
84 device in clinical practice<sup>8,9</sup>. We report on the test-retest reliability of the binocular OCT for  
85 the measurement of pupil parameters and its ability to detect RAPD in healthy volunteers  
86 and patients diagnosed with RAPD, where SFM was used as the reference standard.

1  
2 **87 Methods**  
3  
4

5 **88**

---

7  
8 **89** Approval for prospective data collection and analysis was obtained from a UK National Health  
9  
10 **90** Service Research Ethics Committee (London-Central) as part of the PUPIL study  
11  
12 **91** (ClinicalTrials.gov Identifier: NCT03081468). Written informed consent was obtained from all  
13  
14 **92** participants. The study adhered to the tenets set forth in the Declaration of Helsinki.

15  
16  
17 **93** Fifty participants with eye disease with a positive RAPD confirmed using SFM by their  
18  
19 **94** treating clinician and a study investigator (RC) were recruited from emergency, glaucoma,  
20  
21 **95** medical retina, and neuro-ophthalmology clinics at Moorfields Eye Hospital, London. Fifty  
22  
23 **96** healthy participants with a self-reported normal ocular examination within the previous year and  
24  
25 **97** an absent RAPD on SFM were also recruited. As a ratio of the constriction amplitude is used to  
26  
27 **98** calculate RAPD (as described below), the subject's fellow eye serves as a control, and therefore  
28  
29 **99** participants were not age or sex matched<sup>10</sup>.

30  
31  
32 **100** Individuals were excluded if they had any significant ocular opacity or ptosis that  
33  
34 **101** obscured visibility of the pupil; if they had any ocular, neurological, or systemic disease that  
35  
36 **102** might affect the efferent limb of the pupil pathway; or if they were using any systemic or topical  
37  
38 **103** medications known to alter pupil size, such as pilocarpine or opiates. Preliminary testing  
39  
40 **104** involved visual acuity measurement using the logarithmic visual acuity chart (logMAR) with  
41  
42 **105** habitual correction. All visual field tests were undergone on a Humphrey Visual Field Analyzer  
43  
44 **106** (Carl-Zeiss Meditec, USA) using the SITA 24-2 algorithm. Habitual refractive error correction  
45  
46 **107** was measured using a lensmeter to determine a best spherical equivalent for correction within  
47  
48 **108** the binocular OCT device to aid visibility of the fixation target. The mean deviation (MD) results  
49  
50 **109** from the participants' visual field test (<6 months) were recorded.  
51

52  
53  
54 **110**

55  
56  
57 **111 RAPDx examination**  
58  
59  
60  
61  
62  
63  
64  
65

112 Participants underwent a single examination using the RAPDx device (Konan Medical USA,  
113 Irvine, CA, USA), an automated infrared pupillometer. Each participant was tested in a dimly-lit  
114 room (<5 lux) and dark-adapted for 2-3 minutes prior to examination as recommended in the  
115 manufacturer's user manual. The participant placed their head against the RAPDx device  
116 interface that blocks out the majority of external illumination. The RAPDx presents bright white  
117 stimuli monocularly covering a field of view of 30-degrees. The stimulus alternates between the  
118 eyes, while the subject continues to view a nominal white background and fixation target as a  
119 cyclopean scene. The stimuli were presented for 0.2s duration, with 1.9s between each  
120 stimulus. The results from the first pair of stimuli are discarded. The device continues to present  
121 visual stimuli until 8 pairs of recordings are obtained. If the device records a blink during the  
122 pupil recording, the pair is automatically repeated. The recordings are averaged to output a  
123 constriction 'amplitude' and 'latency' RAPD score. The amplitude score was used for this study  
124 as a comparable parameter to that produced by the binocular OCT.

125 Raw data for other pupil parameters was obtained from the manufacturer for analysis.

126 The RAPD measurement was calculated using the mean pupil constriction amplitudes for each  
127 eye.

128

### 129 **Binocular OCT examination**

130 The specifications of the device are described elsewhere<sup>8</sup>. Briefly, this device acquires OCT  
131 images of the 'whole-eye' in a single instrument. The display screens within the device can be  
132 customized, and for this study displayed a single controlled flash of white light to each eye whilst  
133 simultaneously capturing OCT scans of the anterior segments including the iris plane of both  
134 eyes.

135 Each participant was dark-adapted for 2-3 minutes prior to binocular OCT pupillometry  
136 examination. The machine is light-proof, blocking out all external light when users place their  
137 head within the mask-machine interface. To assess repeatability (test-retest variability),  
138 participants underwent two trials on the binocular OCT within the same session, separated by a  
139 minimum interval of 15 minutes. The binocular OCT ensures alignment and visualization of the

140 pupils prior to stimulus presentation as described previously. The OCT captures pupillary  
141 images of both eyes every 47ms for 350ms prior to the stimulus, and 4s after stimulus  
142 presentation. The left eye is first presented with a fixation target on a black background, and is  
143 stimulated with a bright flash of white light of 38x20 degrees with a luminance of 25cd/m<sup>2</sup> for  
144 0.25s duration. The fixation target is then presented to the right eye, with realignment of the  
145 oculars if necessary. Once aligned, the same controlled stimulus is presented to the right eye.  
146 From these images, the pupil margins can be determined, and a circumference measurement  
147 can be derived as described below. The binocular OCT generates similar parameters to the  
148 RAPDx. These can be used to calculate the constriction amplitude as a ratio between the eyes  
149 to generate a RAPD value in log units.

150 Pupil metrics are derived using 4 horizontal line scans over the central 3mm of the  
151 anterior segment. Each line scan is separated by 1mm (Figure 1), generating 8 possible  
152 intersections with the pupillary margin. The pupil may occasionally be obstructed in images if it  
153 moves off-center - this is especially related to eye movement during capture. Only 2 line scans  
154 with the pupil visible, i.e. at least 3 pupil margin points, are required to calculate the pupil  
155 diameter by fitting those points to a circle in 3D space, whereas the RAPDx uses an enface 2D  
156 image. When more than 3 pupil margin points are available, a random sample consensus  
157 (RANSAC) algorithm is used to calculate the diameter by fitting circles to 3 points selected at  
158 random. Multiple iterations form a consensus of the best fitting circle.

159

## 160 **Data Analysis and Statistics**

161 The following pupil parameters were compared for test-retest reliability:

- 162 ● Maximum/resting pupil diameter (mm)
- 163 ● Minimum pupil diameter (mm)
- 164 ● Anisocoria (defined as the difference in pupil diameter between eyes and measured in  
165 the 0.5 seconds before stimulus presentation) (mm)
- 166 ● Constriction amplitude using maximum and minimum pupil diameter (%)



- 167 • RAPD (log units) calculated using the following formula, where a positive result indicates  
168 a right RAPD and a negative result indicates a left RAPD:

$$RAPD = 10\log_{10}\left(\frac{\text{constriction amplitude left eye}}{\text{constriction amplitude right eye}}\right)$$

169  
170 Diagnostic accuracy of each device was assessed compared to the SFM, which was  
171 used as the ground truth. Receiver operating characteristic curves (ROC) were used for  
172 sensitivity and specificity analysis using an absolute value of the RAPD score. Agreement  
173 between binocular OCT trials were appraised using the intraclass correlation coefficient for test-  
174 retest reliability. Bland-Altman graphs were used for intra- and inter-device comparisons.  
175 Proportional bias was assessed using linear regression analysis plotted on the Bland-Altman  
176 graphs.

177 To assess the correlation between RAPD score and visual function, Pearson's  
178 correlation coefficient and  $R^2$  values from univariable linear regression were used. Inter-eye  
179 differences were computed left eye minus right eye values for MD and logMAR visual acuity.

180 Independent t-tests were used to assess statistically significant differences in  
181 demographics and pupil parameters between the healthy and disease groups. Paired t-tests  
182 were used to assess intra- and inter-device differences. A P-value of  $\leq 0.05$  was considered to  
183 be statistically significant.

## 184 Results

185

---

186 The mean age of the cohort with eye disease and a positive RAPD was 49.6 years (interquartile  
187 range (IQR): 35-60.5 years), and 52% were female. A summary of the range of eye diseases in  
188 this cohort are presented in Table 1. The fifty healthy participants had a mean age of 31.3 years  
189 (IQR: 25 to 32 years), and 58% were females. Age, visual acuity in the worse eye, and  
190 refractive error were significantly different between the two groups ( $P \leq 0.05$ ).

191 All participants completed both examinations on the binocular OCT, amounting to 100  
192 participants and 200 examinations. One healthy volunteer and one participant with a positive  
193 RAPD did not complete the RAPDx examination due to excessive blinking and unreliable  
194 detection of the pupil due to a co-existing peripheral iridotomy, respectively. Therefore 49  
195 healthy controls and 49 participants with RAPD were used for comparison of the binocular OCT  
196 with the RAPDx.

197 The binocular OCT examination generates a series of images that can be collated into a  
198 video - an example of a participant with a positive right RAPD is presented in Supplementary  
199 Video 1 (available online at [URL]). A summary is shown in Figure 2. A quantitative pupillometry  
200 report for each participant is generated at the end of the examination, providing a data-rich  
201 analysis of the examination (Figure 3).

202

### 203 Test-retest reliability and intra- and inter-device agreement

204 The following pupil parameters were analyzed for test-retest reliability using the intraclass  
205 correlation coefficient (ICC): maximum and minimum pupil diameters, anisocoria, constriction  
206 amplitude. Pupil diameters from both direct and consensual responses for both healthy and  
207 diseased cohorts were aggregated to form a list of 400 test-retests from 100 participants. The  
208 intraclass correlation coefficient (ICC) for OCT-derived maximum pupil diameter, minimum pupil  
209 diameter, anisocoria, and constriction amplitude was 0.95 (95% confidence interval [CI] 0.94-

210 0.96), 0.93 (CI: 0.91-0.94), 0.97 (CI: 0.95-0.97), and 0.88 (CI: 0.85-0.90), respectively. For  
211 RAPD measurement, the ICC was 0.90 (CI: 0.74-0.87). Minimum pupil diameter, absolute pupil  
212 constriction and constriction amplitude were significantly different between the tests for both  
213 cohorts, however RAPD measurements were not (Table 2; paired t-test).

214 Intra- and inter-device agreement is shown in Bland-Altman (BA) plots in Figure 4. The  
215 BA plots for both cohorts show a significant proportional bias ( $P < 0.001$ ) for test-retest (Figure  
216 4A-B) but with high variability ( $R^2 = 0.25$ ). This suggests that the RAPD measurements from the  
217 first trial were of larger magnitude compared to the second trial. The limits of agreement had a  
218 smaller range for the healthy participants ( $\pm 1.70$ ) than the cohort with eye disease ( $\pm 2.27$ ). Inter-  
219 device agreement was assessed between the second binocular OCT trial and the RAPDx  
220 (Figure 4C-D). Limits of agreement were smaller for both cohorts in comparison to test-retest  
221 measures, indicating better agreement between the second binocular OCT trial and the RAPDx.  
222 The distribution of measured RAPD is illustrated in the violin plots in Figure 5, showing a tighter  
223 distribution in the second trial compared to the first trial, with fewer observed outliers. The  
224 measured scores on the RAPDx show an even tighter distribution for the healthy cohort in  
225 comparison to the binocular OCT.

226 Paired t-tests showed nearly all pupil parameters were significantly different between the  
227 two devices for both groups, as expected due to the different light conditions. RAPD  
228 measurements were not statistically different between the devices and groups (Table 2).

### 230 **Diagnostic accuracy for RAPD detection**

231 Results for the second examination on the binocular OCT were used for comparison with the  
232 RAPDx. For healthy participants, the mean (SD) RAPD score was +0.01 ( $\pm 0.21$ ) log units (95%  
233 CI: -0.05 to 0.06) using the RAPDx. In comparison, the mean (SD) RAPD score for this cohort  
234 using binocular OCT was 0.04 ( $\pm 0.54$ ) log units (95% CI: -0.19 to 0.12). For participants with  
235 eye disease, the mean (SD) RAPD score was -0.0002 ( $\pm 2.13$ ) log units (95% CI: -0.61 to 0.61)  
236 using the RAPD, and +0.07 ( $\pm 1.97$ ) log units (95% CI: -0.49 to 0.63) using binocular OCT. The  
237 RAPDx and binocular OCT agreed on which eye was affected for all participants in the diseased

1  
2  
3  
4  
5  
6  
7  
8  
9  
10  
11  
12  
13  
14  
15  
16  
17  
18  
19  
20  
21  
22  
23  
24  
25  
26  
27  
28  
29  
30  
31  
32  
33  
34  
35  
36  
37  
38  
39  
40  
41  
42  
43  
44  
45  
46  
47  
48  
49  
50  
51  
52  
53  
54  
55  
56  
57  
58  
59  
60  
61  
62  
63  
64  
65

238 cohort. In the healthy cohort, the RAPDx and binocular OCT agreed on the affected side in 29  
239 participants (59%).

240 Absolute values of the RAPD scores were used to measure diagnostic accuracy, with  
241 the caveat that this does not take into account whether the instrument correctly identifies the  
242 RAPD on the affected eye. The area under the ROC curve (AUC) for the RAPDx device was  
243 0.963, indicating excellent diagnostic ability when using SFM as the reference standard (Figure  
244 6). The AUC for binocular OCT was 0.832, indicating good diagnostic ability but inferior to the  
245 RAPDx. The threshold to detect disease whilst optimizing for both sensitivity and specificity was  
246 between 0.4 and 0.5 log units for both the RAPDx and binocular OCT. At a threshold of 0.5 log  
247 units, the RAPDx had a sensitivity of 82% and a specificity of 94% for detection of RAPD,  
248 whereas the binocular OCT had a sensitivity of 74% and specificity of 86%. The diagnostic  
249 accuracy of the RAPDx and binocular OCT was 88% (CI: 80-94%) and 80% (CI: 71-87%)  
250 respectively. At the 0.3 log units threshold, the RAPDx and binocular OCT sensitivity/specificity  
251 was 92/89% and 86/66%, respectively.

1  
2  
3  
4  
5  
6  
7  
8  
9  
10  
11  
12  
13  
14  
15  
16  
17  
18  
19  
20  
21  
22  
23  
24  
25  
26  
27  
28  
29  
30  
31  
32  
33  
34  
35  
36  
37  
38  
39  
40  
41  
42  
43  
44  
45  
46  
47  
48  
49  
50  
51  
52  
53  
54  
55  
56  
57  
58  
59  
60  
61  
62  
63  
64  
65

**252 Correlation of RAPD with visual function parameters in cohort with pathological RAPD**

253 A larger inter-eye difference in mean deviation was associated with a larger RAPD score  
254 measured on the binocular OCT (correlation coefficient  $R=0.58$ ,  $P<0.001$ ,  $R^2=0.33$ ), and even  
255 more strongly associated with RAPD score measured on the RAPDx ( $R=0.76$ ,  $P<0.001$ ,  
256  $R^2=0.57$ ). The relationship between visual acuity and RAPD score was similar for both binocular  
257 OCT ( $R=0.74$ ,  $P<0.001$ ,  $R^2=0.54$ ), and RAPDx ( $R=0.77$ ,  $P<0.001$ ,  $R^2=0.59$ ). This suggests a  
258 moderately positive relationship between increasing difference of visual acuity and increasing  
259 RAPD score.

## 260 Discussion

261

---

262 In this study, pupillometry was performed using two devices with two different technologies:  
263 RAPDx, utilizing infrared cameras to image the pupil circumference enface; and a prototype  
264 binocular OCT instrument, employing swept-source lasers to capture high-resolution cross-  
265 sectional images through the iris and pupil planes. To our knowledge, this is the first time that  
266 the binocular pupil responses have been assessed using OCT imaging.

267 Binocular OCT pupillometry was found to have excellent test-retest reliability for pupil  
268 parameters such as maximum and minimum pupil diameter, and anisocoria. Although  
269 constriction amplitude performed well on ICC testing, agreement was slightly lower than the  
270 other measured parameters. As constriction amplitude is calculated using pupil diameter values,  
271 small errors in maximum and minimum pupil diameters can propagate error into constriction  
272 amplitude measurement, and consequently RAPD calculation. In addition, the distribution of  
273 RAPD was found to be wider for the first trial compared to the second trial although the  
274 distributions were not statistically significant. This suggests there may be a learning effect as the  
275 user becomes familiar with the device, the fixation target, and how bright the flash will be,  
276 reducing measurement error on subsequent trials. This effect is demonstrated in other devices  
277 such as perimetry, where fixation and thus test-retest variability improves upon repeat testing<sup>11-</sup>  
278 <sup>13</sup>. Further testing eliminating potential learning effect errors should be carried out in future work  
279 to understand the extent to which this and other artefacts contributes to test-retest variability,  
280 which may limit the application of such a RAPD measure in clinical practice.

281 Although the diagnostic accuracy for RAPD detection was inferior to the RAPDx, OCT-  
282 derived measurements show promise in detecting these, often subtle, abnormalities. Literature  
283 evidence suggests that a RAPD score of within  $\pm 0.3$  log units is physiological, whereas a  
284 threshold of  $\pm 0.5$  log units is suggested as a cut-off to detect disease<sup>10,14,15</sup>, in agreement with  
285 our findings - the optimum threshold for disease detection using the binocular OCT was 0.5 log  
286 units. However, the specificity of the binocular OCT was worse than the RAPDx at a threshold

287 of 0.3 log units, recommended as the threshold for presence of a physiological RAPD. We  
288 hypothesize that diagnostic accuracy is affected by small eye movements during OCT capture  
289 that may cause the pupil to become occluded in one or more B-scans, thus reducing the  
290 number of possible iterations of the RANSAC algorithm used to calculate the ratio of constriction  
291 amplitude. As a result of fewer iterations, the accuracy of the pupil diameter measurement  
292 reduces. The maximum pupil diameter captured pre-stimulus had slightly better test-retest  
293 reliability than minimum pupil diameter - generally measured 1-2 seconds later, when the eyes  
294 have had the opportunity to move. One advantage of measuring the pupils using OCT is that  
295 RANSAC utilizes 3-dimensional space, whereas the RAPDx and other infrared pupillometers  
296 use a 2-dimensional enface measurement only. This might be helpful in eyes with strabismus<sup>9</sup>.

297 For this study, we used SFM as the reference standard for detecting the presence or  
298 absence of RAPD. Despite its flaws, the SFM is still the most commonly used pupillometry  
299 assessment in clinical practice. As a result, false positives and false negatives are likely to  
300 occur. In 4 participants with RAPD confirmed by SFM, both the RAPDx and binocular OCT  
301 measured a RAPD within  $\pm 0.5$  log units, and therefore below the threshold for disease  
302 detection. Although participants were confirmed with RAPD using the SFM by a trained  
303 observer, it is possible that some of these cases were false positives. On follow-up of case  
304 notes for these patients, two participants had a diagnosis of optic neuritis 6 months prior to  
305 testing and had made a recovery from all other symptoms; and one participant had asymmetric  
306 primary open angle glaucoma with a difference in MD of 6dB between the eyes which may not  
307 elicit an RAPD on quantitative testing<sup>16</sup>. Another participant had a healthy optic disc in the right  
308 eye, and normal tension glaucoma (NTG) in the left eye, with a difference of 0.18 in visual acuity  
309 and -16.7 in MD, but only measured a left RAPD of 0.20 and 0.26 log units on the binocular  
310 OCT and RAPDx, respectively. This case is likely to be a false negative, however recent  
311 literature has shown that those with NTG have a lesser RAPD for a given inter-eye difference in  
312 MD compared to those with open angle glaucoma<sup>17</sup>. These cases further support the need for  
313 objective methods of performing pupillometry.

1  
2  
3  
4  
5  
6  
7  
8  
9  
10  
11  
12  
13  
14  
15  
16  
17  
18  
19  
20  
21  
22  
23  
24  
25  
26  
27  
28  
29  
30  
31  
32  
33  
34  
35  
36  
37  
38  
39  
40  
41  
42  
43  
44  
45  
46  
47  
48  
49  
50  
51  
52  
53  
54  
55  
56  
57  
58  
59  
60  
61  
62  
63  
64  
65

314 In line with previous literature, we found a positive relationship between inter-eye  
315 difference in MD and RAPD score measured by both devices<sup>17-20</sup>. Interestingly, we found that  
316 there was also an association between visual acuity and RAPD score. Although contradictory  
317 results have been reported in the other studies<sup>21-23</sup>, it is not surprising that RAPD was found in  
318 the eye with the worse visual acuity.

319 The binocular OCT pupillometry exam has several limitations at present. The RAPDx  
320 averages 8 pairs of measurements to minimize noise and the effect of anomalies, whereas the  
321 binocular OCT only uses a single measurement. This difference in methodology means the test  
322 duration is shorter for the binocular OCT device, which may be worthwhile in busy clinic.  
323 However, the signal/noise ratio is poorer, resulting in greater measurement scatter and may  
324 increase the impact of random error<sup>22</sup>. In addition, the difference in stimulus characteristics  
325 between the devices such as stimulus luminance are likely to elicit a different magnitude of pupil  
326 response. These are likely to be a major factors in explaining the underperformance in  
327 diagnostic accuracy of the binocular OCT when compared with the RAPDx. Future iterations of  
328 the device should allow rapid repetitive stimulation of the pupils, and should follow stimulus  
329 characteristics as recommended by Kelbsch et al.<sup>24</sup>. In this work we focus on amplitude  
330 measurements to calculate RAPD, however latency measures can also be used. Velocity and  
331 amplitude of the pupil light reflex are linearly related<sup>25</sup>, so there is no a priori reason to expect  
332 any additional information from latency measures as an outcome measure. However, the  
333 sampling frequency of the OCT should be improved upon in future iterations for accurate  
334 velocity and latency measures that are often informative for other pupil abnormalities in addition  
335 to RAPD.

336 The binocular optical coherence tomography system has shown promise for automated  
337 OCT imaging<sup>8</sup>, and for novel applications that exploit the binocularity aspect of the device, such  
338 as evaluation of strabismus<sup>9</sup>. In the future, pupillometry - an essential aspect of the eye  
339 examination, could be performed in an automated manner using OCT. Unfortunately, automated  
340 pupilometers such as the Konan RAPDx system are not widely used in clinical practice. This is  
341 largely because they are expensive devices, limited to a single purpose. In the real-world busy



1  
2 342 clinic, the swinging flashlight method is still the test of choice - often performed by technicians  
3  
4 343 who may not be trained observers. . Thus, an automated system that is capable of performing a  
5  
6 344 comprehensive quantitative examination may be more sensitive for disease detection, and may  
7  
8 345 perhaps provide new insights into the pathophysiology of disease.  
9  
10  
11  
12  
13  
14  
15  
16  
17  
18  
19  
20  
21  
22  
23  
24  
25  
26  
27  
28  
29  
30  
31  
32  
33  
34  
35  
36  
37  
38  
39  
40  
41  
42  
43  
44  
45  
46  
47  
48  
49  
50  
51  
52  
53  
54  
55  
56  
57  
58  
59  
60  
61  
62  
63  
64  
65

1  
2  
3 **346 Acknowledgements:**

4 **347** The authors have no financial links with Envision Diagnostics, Inc.

5 **348** Dr. Keane has received speaker fees from Heidelberg Engineering, Topcon, Haag-Streit,  
6  
7 **349** Carl Zeiss Meditec, Allergan, Novartis, and Bayer. He has served on advisory boards for  
8  
9 **350** Novartis and Bayer, and is an external consultant for Optos and Google Health. Dr. Mulholland  
10  
11 **351** and Prof. Anderson have received travel support from Heidelberg Engineering. Dr. Mulholland  
12  
13 **352** receives research support from LKC Technologies, Inc. Dr. Petzold has received speaker fees  
14  
15 **353** and travel support from Heidelberg Engineering. He is on steering committees for Novartis  
16  
17 **354** (OCTiMS study) and ZEISS (Angi network). Ms. Chopra receives studentship support from the  
18  
19 **355** College of Optometrists, UK, and is a paid intern at DeepMind. This study was supported by the  
20  
21 **356** Miss Barbara Mary Wilmot Deceased Discretionary Trust.

22  
23 **357** This report is independent research arising from a Clinician Scientist award (CS-2014-14-023)  
24  
25 **358** supported by the National Institute for Health Research. The views expressed in this publication  
26  
27 **359** are those of the author(s) and not necessarily those of the NHS, the National Institute for Health  
28  
29 **360** Research or the Department of Health.  
30  
31  
32  
33  
34  
35  
36  
37  
38  
39  
40  
41  
42  
43  
44  
45  
46  
47  
48  
49  
50  
51  
52  
53  
54  
55  
56  
57  
58  
59  
60  
61  
62  
63  
64  
65

361 **References**

362

- 
- 363 1. Wilhelm H. Neuro-ophthalmology of pupillary function--practical guidelines. *J Neurol.*  
364 1998;245(9):573-583.
  - 365 2. Meneguette NS, de Carvalho JER, Petzold A. A 30 s test for quantitative assessment of a  
366 relative afferent pupillary defect (RAPD): the infrared pupillary asymmetry (IPA). *J Neurol.*  
367 2019;266(4):969-974.
  - 368 3. Martínez-Ricarte F, Castro A, Poca MA, et al. Infrared pupillometry. Basic principles and  
369 their application in the non-invasive monitoring of neurocritical patients. *Neurología (English*  
370 *Edition)*. 2013;28(1):41-51.
  - 371 4. AMERICAN ACADEMY OF OPHTHALMOLOGY. *2019-2020 BASIC AND CLINICAL*  
372 *SCIENCE COURSE, SECTION 05: Neuro-Ophthalmology*. American Academy of  
373 Ophthalmology; 2019.
  - 374 5. Baikoff G, Lutun E, Ferraz C, Wei J. Static and dynamic analysis of the anterior segment  
375 with optical coherence tomography. *J Cataract Refract Surg.* 2004;30(9):1843-1850.
  - 376 6. Cheung CY-L, Liu S, Weinreb RN, et al. Dynamic analysis of iris configuration with anterior  
377 segment optical coherence tomography. *Invest Ophthalmol Vis Sci.* 2010;51(8):4040-4046.
  - 378 7. Walsh AC. Binocular optical coherence tomography. *Ophthalmic Surg Lasers Imaging.*  
379 2011;42 Suppl:S95-S105.
  - 380 8. Chopra R, Mulholland PJ, Dubis AM, Anderson RS, Keane PA. Human Factor and Usability  
381 Testing of a Binocular Optical Coherence Tomography System. *Transl Vis Sci Technol.*  
382 2017;6(4):16.
  - 383 9. Chopra R, Mulholland PJ, Tailor VK, Anderson RS, Keane PA. Use of a Binocular Optical  
384 Coherence Tomography System to Evaluate Strabismus in Primary Position. *JAMA*  
385 *Ophthalmol.* 2018;136(7):811-817.
  - 386 10. Satou T, Goseki T, Asakawa K, Ishikawa H, Shimizu K. Effects of Age and Sex on Values  
387 Obtained by RAPDx® Pupillometer, and Determined the Standard Values for Detecting  
388 Relative Afferent Pupillary Defect. *Transl Vis Sci Technol.* 2016;5(2):18.
  - 389 11. Heijl A, Lindgren G, Olsson J. The effect of perimetric experience in normal subjects. *Arch*  
390 *Ophthalmol.* 1989;107(1):81-86.
  - 391 12. Heijl A, Bengtsson B. The effect of perimetric experience in patients with glaucoma. *Arch*  
392 *Ophthalmol.* 1996;114(1):19-22.
  - 393 13. Wild JM, Dengler-Harles M, Searle AE, O'Neill EC, Crews SJ. The influence of the learning  
394 effect on automated perimetry in patients with suspected glaucoma. *Acta Ophthalmol.*  
395 1989;67(5):537-545.
  - 396 14. Wilhelm H, Peters T, Lütke H, Wilhelm B. The prevalence of relative afferent pupillary  
397 defects in normal subjects. *J Neuroophthalmol.* 2007;27(4):263-267.

- 398 15. Kawasaki A, Moore P, Kardon RH. Variability of the relative afferent pupillary defect. *Am J*  
1 399 *Ophthalmol.* 1995;120(5):622-633.  
2
- 3 400 16. Tatham AJ, Meira-Freitas D, Weinreb RN, Zangwill LM, Medeiros FA. Detecting glaucoma  
4 401 using automated pupillography. *Ophthalmology.* 2014;121(6):1185-1193.  
5
- 6 402 17. Lawlor M, Quartilho A, Bunce C, et al. Patients With Normal Tension Glaucoma Have  
7 403 Relative Sparing of the Relative Afferent Pupillary Defect Compared to Those With Open  
8 404 Angle Glaucoma and Elevated Intraocular Pressure. *Invest Ophthalmol Vis Sci.*  
9 405 2017;58(12):5237-5241.  
10
- 11 406 18. Chang DS, Boland MV, Arora KS, Supakontanasan W, Chen BB, Friedman DS. Symmetry  
12 407 of the pupillary light reflex and its relationship to retinal nerve fiber layer thickness and  
13 408 visual field defect. *Invest Ophthalmol Vis Sci.* 2013;54(8):5596-5601.  
14  
15
- 16 409 19. Sarezky D, Volpe NJ, Park MS, Tanna AP. Correlation Between Inter-Eye Difference in  
17 410 Average Retinal Nerve Fiber Layer Thickness and Afferent Pupillary Response as  
18 411 Measured by an Automated Pupillometer in Glaucoma. *J Glaucoma.* 2016;25(3):312-316.  
19
- 20 412 20. Sarezky D, Krupin T, Cohen A, Stewart CW, Volpe NJ, Tanna AP. Correlation between  
21 413 intereye difference in visual field mean deviation values and relative afferent pupillary  
22 414 response as measured by an automated pupillometer in subjects with glaucoma. *J*  
23 415 *Glaucoma.* 2014;23(7):419-423.  
24  
25
- 26 416 21. Fison PN, Garlick DJ, Smith SE. Assessment of unilateral afferent pupillary defects by  
27 417 pupillography. *Br J Ophthalmol.* 1979;63(3):195-199.  
28
- 29 418 22. Bobak SP, Goodwin JA, Guevara RA, Arya A, Grover S. Predictors of visual acuity and the  
30 419 relative afferent pupillary defect in optic neuropathy. *Doc Ophthalmol.* 1998;97(1):81-95.  
31
- 32 420 23. Thompson HS, Montague P, Cox TA, Corbett JJ. The relationship between visual acuity,  
33 421 pupillary defect, and visual field loss. *Am J Ophthalmol.* 1982;93(6):681-688.  
34
- 35 422 24. Kelbsch C, Strasser T, Chen Y, et al. Standards in Pupillography. *Front Neurol.*  
36 423 2019;10:129.  
37
- 38 424 25. Bremner FD. Pupillometric evaluation of the dynamics of the pupillary response to a brief  
39 425 light stimulus in healthy subjects. *Invest Ophthalmol Vis Sci.* 2012;53(11):7343-7347.  
40  
41  
42  
43  
44  
45  
46  
47  
48  
49  
50  
51  
52  
53  
54  
55  
56  
57  
58  
59  
60  
61  
62  
63  
64  
65

## 426 **Figure Legends**

1  
2  
3 427 **Figure 1.** Position of horizontal line scans acquired through the iris-pupil planes during  
4  
5  
6 428 pupillometry examination are 1mm apart. The pupil margin in each of these scans (shown by a  
7  
8 429 red dot) is used to calculate the pupil diameter using the random sample consensus (RANSAC)  
9  
10 430 method.

11  
12 431  
13  
14  
15 432 **Figure 2.** (A) Resting diameters pre-stimulus; (B) Flash presented to the left eye, constriction of  
16  
17 433 both pupils observed; (C) Both pupils dilate to their resting diameter; (D) Flash presented to the  
18  
19 434 right eye. Constriction amplitude of both eyes is less than that observed when the flash was  
20  
21 435 presented to the left eye.

22  
23 436  
24  
25 437 **Figure 3.** The binocular OCT pupillometry report displays a graphical output of the pupil  
26  
27 438 diameter versus time, and quantitative measurements such as diameters and velocities.

28  
29 439  
30  
31 440 **Figure 4.** (A) and (B): Intra-device agreement. Bland-Altman graphs for healthy participants  
32  
33 441 (left) and participants with disease (right) to assess the agreement between the two binocular  
34  
35 442 OCT trials. (C) and (D): Inter-device agreement between the binocular OCT and RAPDx. Limits  
36  
37 443 of agreement ( $\pm 1.96$  standard deviation) and the mean is shown as dashed lines with shaded  
38  
39 444 confidence intervals. Regression lines are plotted to highlight proportional bias.

40  
41 445  
42  
43  
44  
45 446 **Figure 5.** Violin plots illustrating the distribution of measured RAPD scores by cohort and  
46  
47 447 device.

48  
49 448  
50  
51 449 **Figure 6.** Receiver operating characteristic (ROC) curves showing the ability to discriminate  
52  
53 450 between positive and negative RAPD using the RAPDx (blue) and binocular OCT (red). The  
54  
55 451 area under the curve (AUC) is greater for RAPDx (AUC 0.963) than binocular OCT (AUC  
56  
57 452 0.832). Operating points at 0.3, 0.4, and 0.5 log units are indicated by green markers. The  
58  
59  
60  
61  
62  
63  
64  
65

1 453 optimal threshold for disease detection for both RAPDx and binocular OCT appears to be  
2 454 between 0.4 to 0.5 log units.

3  
4 455

5  
6 456 **Clip 1.** Pupilometry using the binocular coherence tomography system  
7  
8  
9

10  
11  
12  
13  
14  
15  
16  
17  
18  
19  
20  
21  
22  
23  
24  
25  
26  
27  
28  
29  
30  
31  
32  
33  
34  
35  
36  
37  
38  
39  
40  
41  
42  
43  
44  
45  
46  
47  
48  
49  
50  
51  
52  
53  
54  
55  
56  
57  
58  
59  
60  
61  
62  
63  
64  
65

Table\_2

	Healthy (n = 50) vs Disease (n = 50) Independent t-test P-value					
Age (years) - Mean (SD)	0.001					
Sex (% female)	0.356					
Visual acuity worse eye (logMAR) - Mean (SD)	<0.001					
Visual acuity better eye (logMAR) - Mean (SD)	0.761					
Refractive error, mean spherical equivalent (dioptries) - Mean (SD)	0.032					
	Healthy vs Disease Independent t-test P-value		Binocular OCT test-retest Paired t-test P-value		Binocular OCT vs RAPDx Paired t-test P-value	
	Binocular OCT n = 50	RAPDx n = 49	Healthy n = 50	Disease n = 50	Healthy n = 49	Disease n = 49
Maximum pupil diameter (mm) - Mean (SD)	0.202	0.710	0.824	All eyes 0.789 Affected eyes 0.870 Unaffected eyes 0.659	<0.001	All eyes <0.001 Affected eyes <0.001 Unaffected eyes <0.001
Minimum pupil diameter (mm) - Mean (SD)	0.458	0.592	<0.001	All eyes 0.009 Affected eyes 0.054 Unaffected eyes 0.066	<0.001	All eyes <0.001 Affected eyes <0.001 Unaffected eyes <0.001
Anisocoria (mm) - Mean (SD)	0.043	Not reported	0.673	0.173	-	-
Absolute pupil constriction (mm) - Mean (SD)	0.003	<0.001	<0.001	All eyes <0.001 Affected eyes 0.003 Unaffected eyes 0.011	<0.001	All eyes <0.001 Affected eyes <0.001 Unaffected eyes <0.001
Constriction amplitude (%) - Mean (SD)	0.001	<0.001	<0.001	All eyes <0.001 Affected eyes 0.002 Unaffected eyes 0.001	0.112	All eyes <0.001 Affected eyes <0.001 Unaffected eyes 0.008
RAPD (log units) - Mean (SD)	<0.001	<0.001	0.487	0.308	0.629	0.661
Absolute RAPD (log units) - Mean (SD)	<0.001	<0.001	0.160	0.240	0.063	0.130

**Table 2.** Statistical significance tests. Independent t-tests were used to assess significant differences between the healthy and disease group. Paired t-tests were used to assess significant differences for intra- and inter-device comparisons. The second test on the binocular OCT was used for inter-device comparisons. Significance is assumed at  $\leq 0.05$ .



Table\_1

	Healthy (n = 50)		Disease (n = 50)	
Age (years) - Mean (SD)	31.3 (10.1)		49.6 (15.9)	
Sex (% female)	58		52	
Eye diseases	No eye disease present		Branch retinal artery occlusion Glaucoma Idiopathic optic neuropathy Ischaemic central retinal vein occlusion Non-arteritic ischaemic optic neuropathy Idiopathic optic atrophy Optic nerve compression Optic neuritis Traumatic optic neuropathy	n=1 n=22 n=2 n=1 n=1 n=2 n=2 n=17 n=2
Visual acuity worse eye (logMAR) - Mean (SD)	-0.05 (0.10)		0.55 (0.73)*	
Visual acuity better eye (logMAR) - Mean (SD)	-0.08 (0.08)		-0.03 (0.12)	
Mean deviation (dB) worse eye - Mean (SD)	Not performed		-14.59 (6.58)**	
Mean deviation (dB) better eye - Mean (SD)	Not performed		-2.65 (0.45)**	
Refractive error, mean spherical equivalent (dioptries) - Mean (SD)	-1.43±2.17		-0.51 (2.21)	
	Binocular OCT n = 50	RAPDx n = 49	Binocular OCT n = 50	RAPDx n = 49
Maximum pupil diameter (mm) - Mean (SD)	6.78 (1.18)	5.87 (0.99)	All eyes 5.80 (1.19) Affected eyes 5.84 (1.18) Unaffected eyes 5.77 (1.20)	All eyes 5.35 (1.00) Affected eyes 5.33 (0.99) Unaffected eyes 5.38 (1.04)
Minimum pupil diameter (mm) - Mean (SD)	4.94 (1.10)	4.21 (0.82)	All eyes 4.32 (1.08) Affected eyes 4.51 (1.12) Unaffected eyes 4.12 (1.00)	All eyes 4.06 (0.87) Affected eyes 4.25 (0.90) Unaffected eyes 4.07 (0.93)
Anisocoria (mm) - Mean (SD)	0.23 (0.19)	Not reported	0.34 (0.28)	Not reported
Absolute pupil constriction (mm) - Mean (SD)	1.84 (0.43)	1.66 (0.34)	All eyes 1.49 (0.47) Affected eyes 1.33 (0.45) Unaffected eyes 1.65 (0.45)	All eyes 1.30 (0.44) Affected eyes 1.09 (0.38) Unaffected eyes 1.30 (0.46)
Constriction amplitude (%) - Mean (SD)	27.59 (6.33)	28.38 (4.31)	All eyes 25.90 (7.38) Affected eyes 23.07 (7.31) Unaffected eyes 29.74 (6.28)	All eyes 24.22 (7.03) Affected eyes 20.42 (6.52) Unaffected eyes 24.42 (7.16)

<b>RAPD (log units) - Mean (SD)</b>	<b>Trial 1</b> 0.142 (0.87) <b>Trial 2</b> 0.036 (0.54)	0.006 (0.21)	<b>Trial 1</b> 0.238 (2.54) <b>Trial 2</b> 0.069 (1.97)	0.0002 (2.13)
<b>Absolute RAPD (log units) - Mean (SD)</b>	<b>Trial 1</b> 0.560 (0.68) <b>Trial 2</b> 0.36 (0.40)	0.140 (0.15)	<b>Trial 1</b> 1.432 (2.10) <b>Trial 2</b> 1.266 (1.50)	1.565 (1.71)

**Table 1.** Participant characteristics. \*Visual acuity for 48 participants - 1 participant had perception of light vision, 1 participant had no perception of light vision. (Counting fingers and hand movements converted to 2.0 and 3.0 logMAR respectively). \*\*Visual fields for 45 participants - test not performed in 5 eyes with vision of counting fingers, hand movements, perception of light, and no perception of light.

Figure 1  
[Click here to download high resolution image](#)

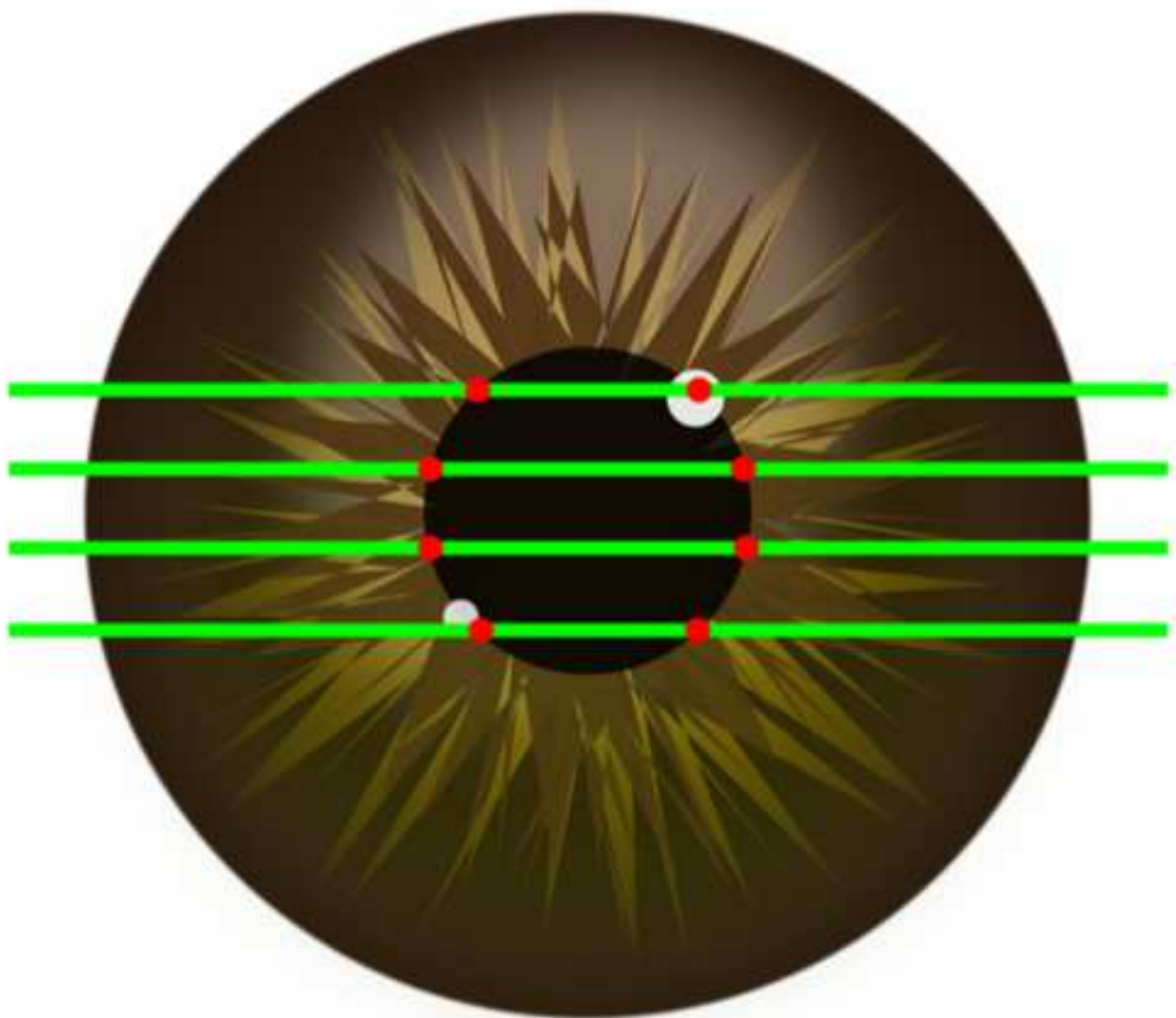


Figure 2  
[Click here to download high resolution image](#)

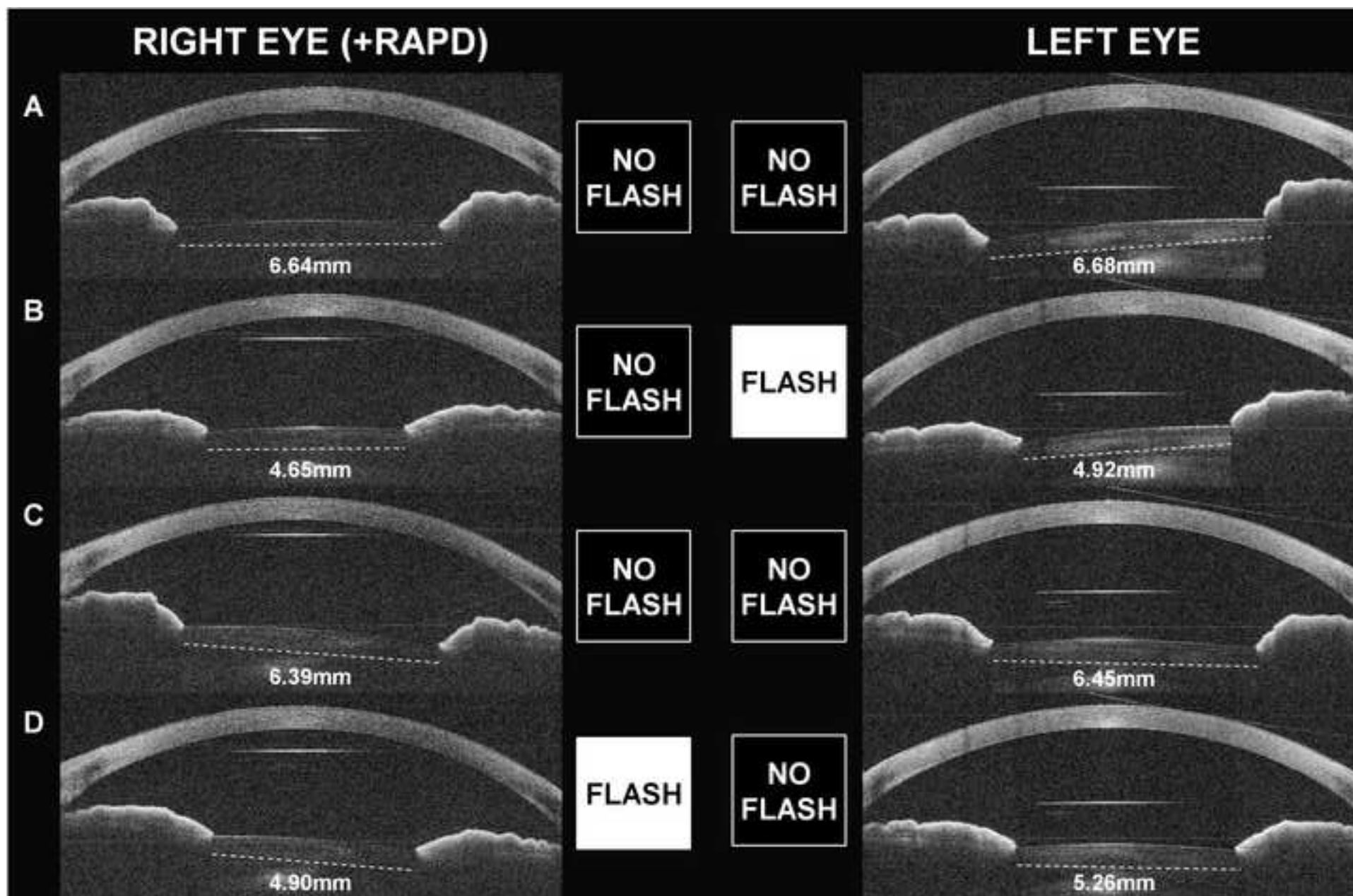
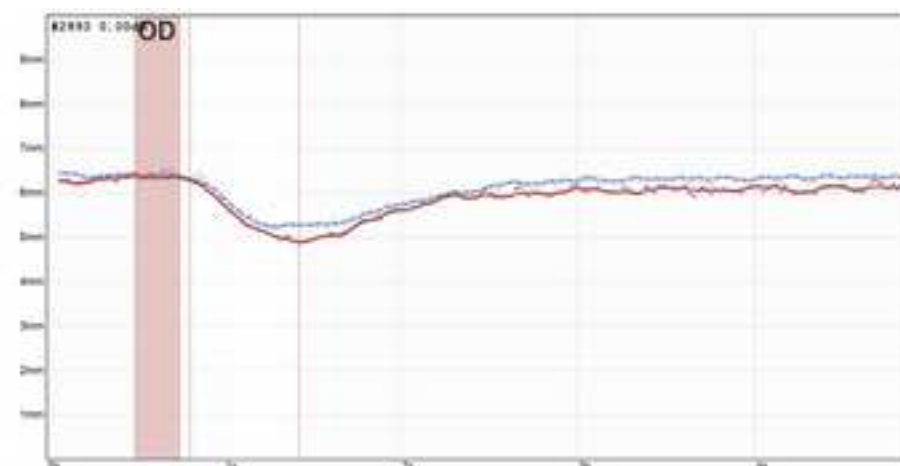
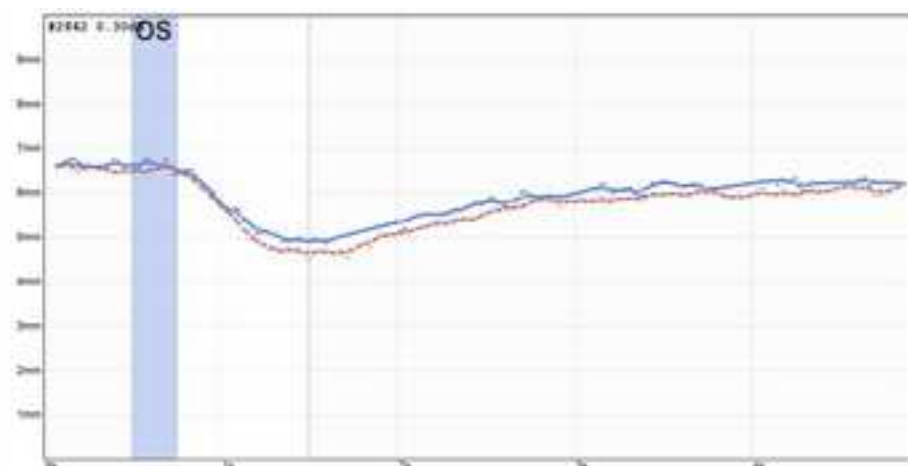


Figure 3

[Click here to download high resolution image](#)



### OS flash

0.19 mm (OS)

-1.46dB (OS)

Anisocoria

RAPD Abs corrected

### OD flash

-0.19 mm (OD)

1.48dB (OD)

Direct (OS)	Consensual (OD)		Consensual (OS)	Direct (OD)
6.68 mm	6.64 mm	<b>Diameter Maximum</b>	6.45 mm	6.39 mm
4.92 mm	4.65 mm	<b>Diameter Minimum</b>	5.26 mm	4.90 mm
1.76 mm	1.99 mm	<b>Constriction Amplitude</b>	1.18 mm	1.48 mm
26 %	30 %	<b>Constriction Amplitude %</b>	18 %	23 %
0.25 s	0.26 s	<b>Constriction Latency</b>	0.26 s	0.31 s
0.75 s	0.88 s	<b>Constriction Duration</b>	0.52 s	0.61 s
4.56 mm/s	4.49 mm/s	<b>Max Constriction Velocity</b>	3.75 mm/s	3.87 mm/s
2.24 mm/s	2.25 mm/s	<b>Avg Constriction Velocity</b>	2.30 mm/s	2.42 mm/s
1.81 mm/s	1.97 mm/s	<b>Max Dilatation Velocity</b>	1.77 mm/s	2.50 mm/s
0.39 mm/s	0.46 mm/s	<b>Avg Dilatation Velocity</b>	0.31 mm/s	0.36 mm/s

**Figure 4**  
[Click here to download high resolution image](#)

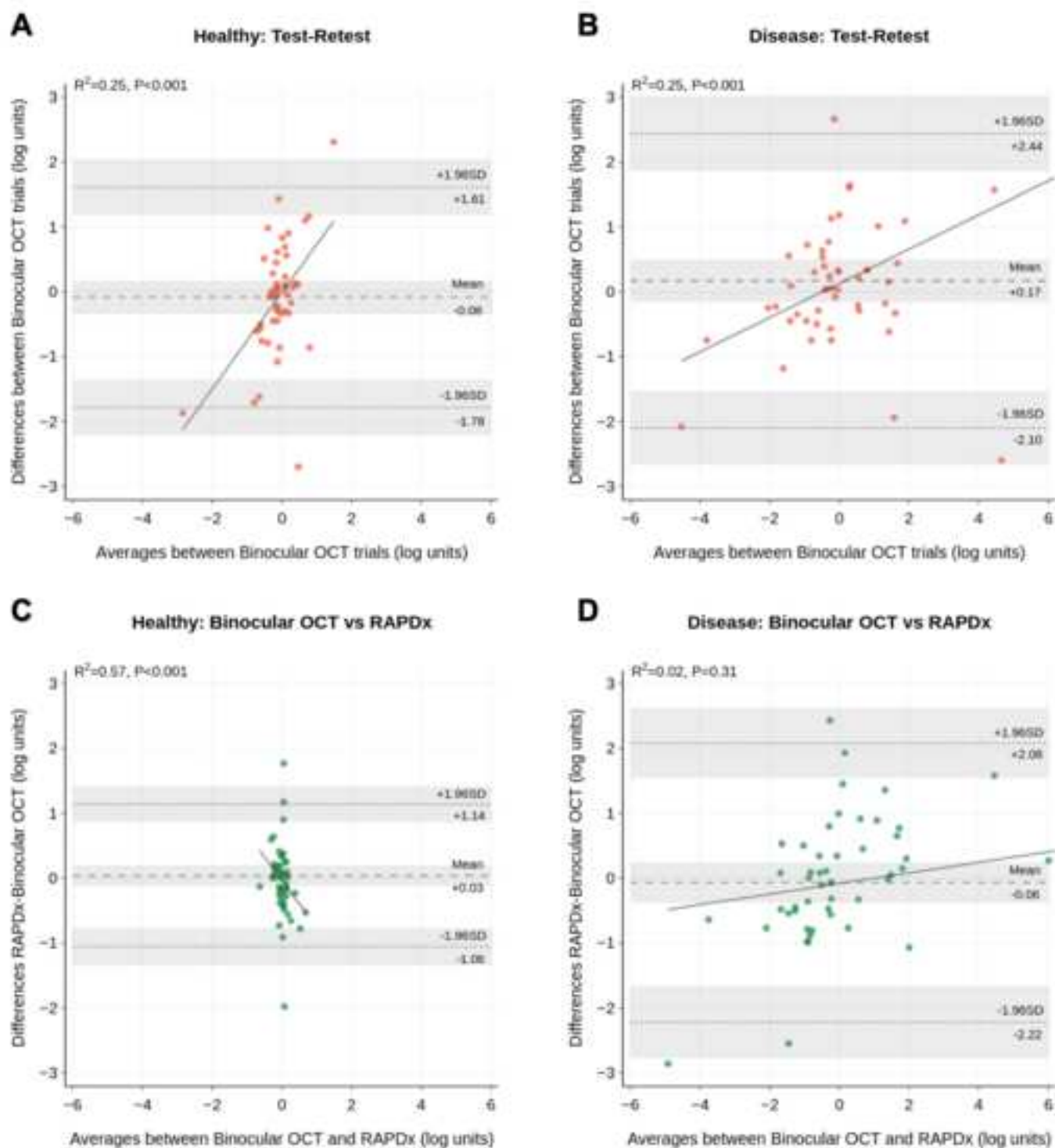


Figure 5  
[Click here to download high resolution image](#)

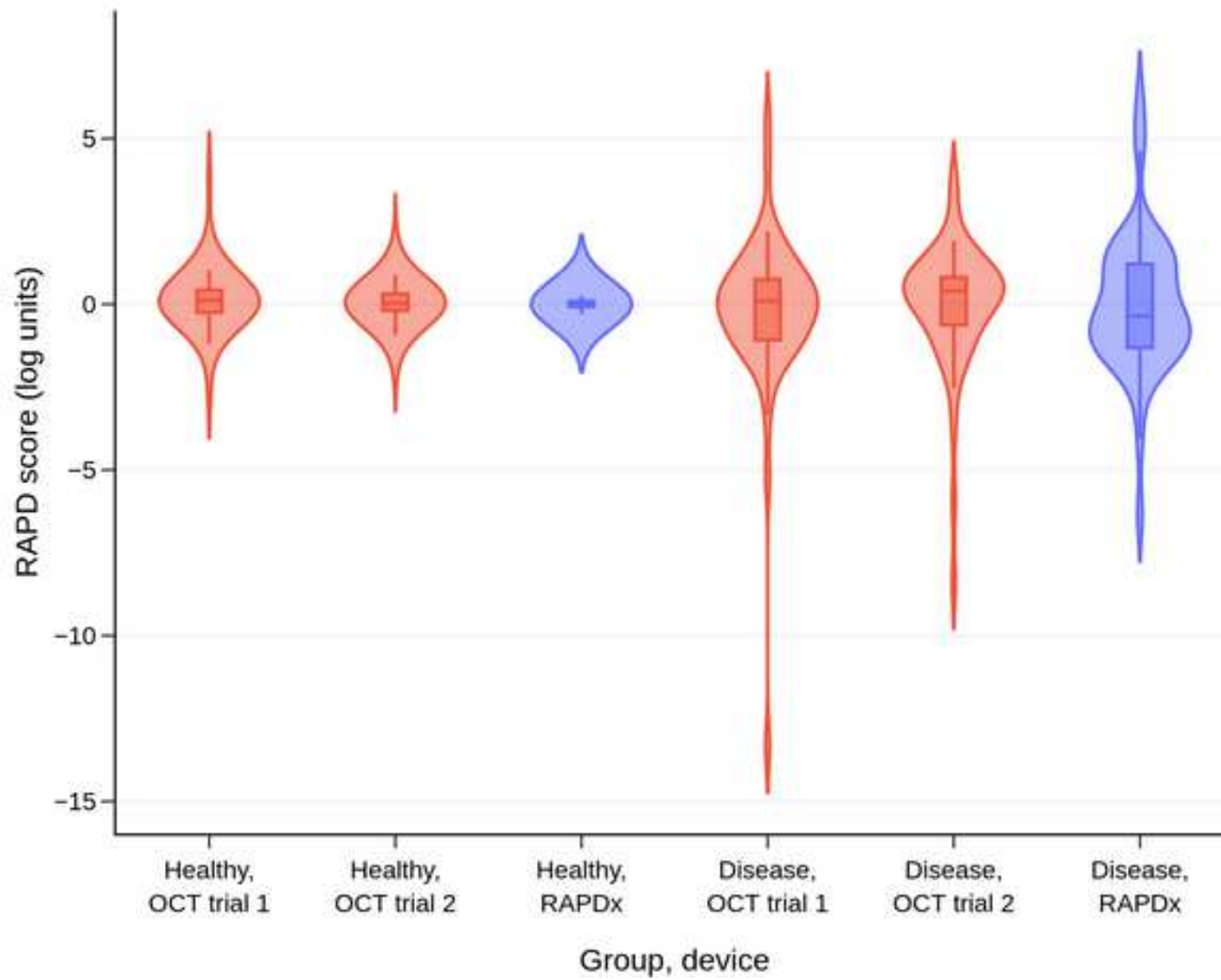
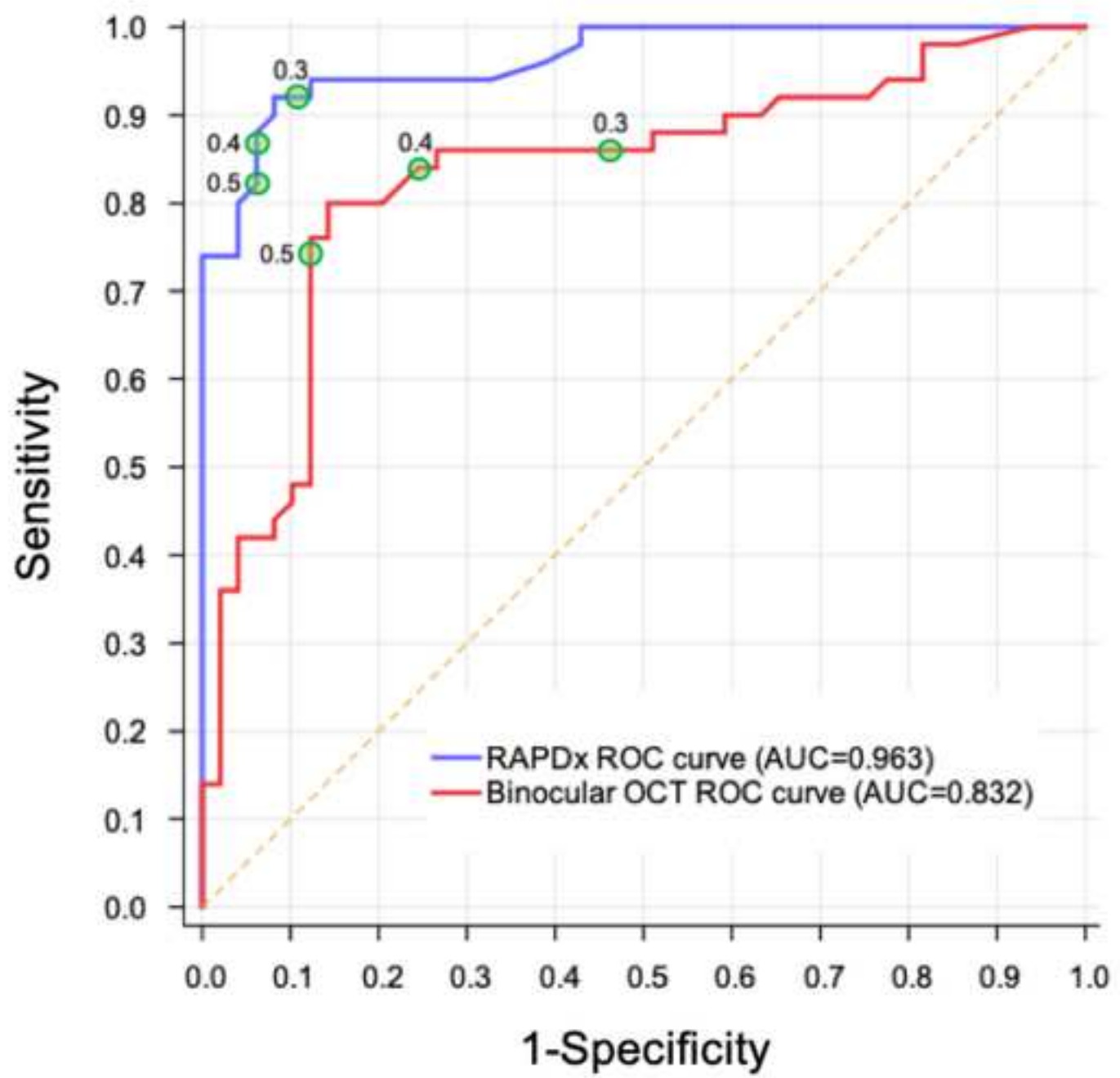




Figure 6  
[Click here to download high resolution image](#)





Video Still

[Click here to download high resolution image](#)

